Electrochemical Immunosensing Chip Using Selective Surface Modification, Capillary-Driven Microfluidic Control, and Signal Amplification by Redox Cycling

Byung-Kwon Kim,[a] *Sang-Youn Yang*,[a] *Md. Abdul Aziz*,[a] *Kyungmin Jo*,[a] *Daekyung Sung*,[b] *Sangyong Jon*,[b] *Han Young Woo*,[c] *Haesik Yang**[a]

[a] Department of Chemistry, Pusan National University, Busan 609-735, Korea
tel: +82 51 510 3681; fax: +82 51 516 7421.:
[b] Department of Life Science, Gwangju Institute of Science and Technology, Gwangju 500-712, Korea
[c] Department of Nanofusion Technology, Pusan National University, Miryang 627-706, Korea
*e-mail: hyang@pusan.ac.kr

Received: February 23, 2010
Accepted: April 2, 2010

Abstract
A sensitive electrochemical immunosensing chip is presented by employing (i) selective modification of protein-resistant surfaces; (ii) fabrication of a stable Ag/AgCl reference electrode; (iii) capillary-driven microfluidic control; (iv) signal amplification by redox cycling along with enzymatic reaction. Purely capillary-driven microfluidic control is combined with electrochemical sandwich-type immunosensing procedure. Selective modification of the surfaces is achieved by chemical reactivity-controlled patterning and electrochemical deposition. Fluidic control of the immunosensing chip is achieved by spontaneous capillary-driven flows and passive washing. The detection limit for mouse IgG in the immunosensing chip is 10 pg/mL.

Keywords: Immunosensor, Passive washing, Microfluidic control, Nonspecific binding, Ag/AgCl reference electrode

DOI: 10.1002/elan.201000148

1. Introduction

Electrochemical detection is considered as one of the major sensing methods in microchip-based biosensors as it facilitates a miniature sensing system [1–6]. Although many different types of electrochemical biosensors that employ large electrodes have been developed, their practical application in microchips remains challenging [1,5–7]. The main reason for this is that the sensitivity and reproducibility obtained with biosensors that use large electrodes cannot be readily achieved with microchip-based biosensors that use micropatterned electrodes. The poor sensitivity and reproducibility associated with microchip-based biosensors is largely due to (i) high nonspecific binding of biomolecules to microchamber and microchannel walls; (ii) low stability of microfabricated reference electrodes; (iii) complex microfluidic control required during the detection process [1,4,6,8,9].

Essentially, microchip-based electrochemical biosensors require at least four different surfaces (working, reference, counter electrode, insulating surface between electrodes) that should be selectively modified and should share high protein-resistant properties. Therefore, a good combination of different protein-resistant surfaces and their sequential selective modification are required for microchip-based electrochemical biosensors. Generally, for selective surface modification, photolithographic patterning [10], electrochemical deposition [11], and chemical reactivity-controlled patterning [12] have been used. Photolithographic patterning and electrochemical deposition are useful in obtaining metal micropatterns, although neither are effective for selective immobilization of (bio)-molecules. However, chemical reactivity-controlled patterning that takes advantage of selective chemical reactivity between a (bio)molecule and a solid surface is useful for selective immobilization of the (bio)molecule [12]. Selective chemical reactivity includes biospecific binding, such as biotin-avidin binding [13,14], and selective chemical reactions, such as selective reaction of an organophosphonate to a metal oxide surface over silicon oxide surface [15,16].

For preparation of protein-resistant surfaces, covalent modification and adsorption-based modifications have been used. Surface modification using a poly(ethylene glycol) (PEG)-containing molecule or polymer is the most common approach towards covalent modification [13,17,18]. Blocking agents such as bovine serum albumin, Tween 20, and skim milk are commonly used for adsorption-based modification [19–21]. Importantly, covalent modifications can be combined with chemical reactivity-controlled patterning.

Microfabricated reference electrodes are essential in microchip-based electrochemical biosensors. Although simple pseudo-reference electrodes such as a micropatterned Au electrode [22,23] can be used, reference electrodes with greater stability are required to achieve biosensors with high reproducibility. Generally, microfabricated Ag/AgCl reference electrodes are most widely used as their exchange current is large and their reference potential is stable [24–26]. In many cases, however, the facile dissolution or stripping of AgCl and the low adhesion properties of Ag on the surface [9,25] make it difficult to achieve a highly stable and reproducible Ag/AgCl reference electrode. Moreover, special care should be taken to obtain a micropattern of Ag and AgCl.

Microfluidic control is essential for heterogeneous phase biosensing in a microchip. Electrokinetic fluid control [27,28] and mechanical fluid control [20,29] have been commonly used for microfluidic control. Nevertheless, microfluidic control based upon capillarity (capillary-driven microfluidic control) offers spontaneous fluid flow [30–32], passive merging [33], and passive washing [34] without using external forces. Capillarity is related to contact angle and configuration of channels [33,34]. Therefore, when selective and protein-resistant surface modifications are designed, the contact angles of the modified surfaces should be considered for capillary-driven microfluidic control; these surfaces should be moderately hydrophilic [34,35]. Moreover, the configuration of channels should be properly designed for passive merging and washing [33,34].

In recent years, this lab has developed highly sensitive electrochemical biosensors using indium tin oxide (ITO) electrodes that offer low and reproducible background-current levels [36–39]. This lab has also shown that signal amplification by redox cycling can significantly lower detection limits of electrochemical biosensors [36,37]. In this study, an electrochemical immunosensing microchip was developed using an ITO electrode and signal amplification by redox cycling. For the first time, purely capillary-driven microfluidic control was combined with electrochemical sandwich-type immunosensing procedure. The microchip consists of an upper plate made of poly(dimethylsiloxane) (PDMS), onto which a microchamber and microchannels were formed, and a lower plate made of a micropatterned ITO glass, onto which biospecific binding and electrochemical detection occurred. To achieve high sensitivity and reproducibility with the microchip-based biosensor, both selective modification of protein-resistant surfaces and a stable microfabricated Ag/AgCl reference electrode were developed. Channel configuration was designed to allow microfluidic control using capillary-driven flow and passive washing. The performance of an immunosensing chip was assessed by determining a detection limit for a target protein, mouse IgG.

2. Experimental

2.1. Reagents and Instruments

Alkaline phosphatase-conjugated antimouse IgG produced in goat (γ-chain specific) (ALP-IgG), biotin-conjugated antimouse IgG (whole molecule) (biotin-IgG), mouse IgG, streptavidin from *Streptomyces avidinii*, fluorescein isothiocyanate-conjugated bovine serum albumin (FITC-BSA), 3-phosphonopropionic acid (PPA), (+)-biotin *N*-hydroxysuccinimide ester, *N*-hydroxysuccinimide (NHS), 1-ethyl-3-[3-(dimethyl-amino)propyl]carbodiimide hydrochloride (EDC), trichloroethylene, ethanol, H_2O_2, NH_4OH, $CrCl_3{\cdot}6H_2O$, $HAuCl_4{\cdot}3H_2O$, Ag_2SO_4, and $FeCl_3$ were purchased from Sigma-Aldrich. 4-Aminophenylphosphate monosodium salt (97%) (APP) was obtained from LKT Laboratories, Inc. (W. St. Falls, MN, USA). All reagents were used without further purification. The PBS solution consisted of 0.01 M phosphate, 0.138 M NaCl, and 0.0027 M KCl (pH 7.4). The PBSB solution contained all of the ingredients of PBS, plus 1% (w/v) bovine serum albumin (pH 7.4). The rinsing buffer (RB) consisted of 50 mM tris(hydroxymethyl)aminomethane, 40 mM HCl, 0.5 M NaCl, and 0.05% (w/v) albumin-bovine serum (pH 7.4). The binding buffer (BB) consisted of PBSB and 0.05% (v/v) Tween 20 (pH 7.4). The tris buffer for the electrochemical experiment comprised 50 mM tris(hydroxymethyl)aminomethane, 10 mM KCl, 1.0 g/L $MgCl_2$, and 7.0 mM HCl (pH 9.0). 2% ferrocenyl-tethered dendrimer (Fc-D) [37] and poly(ethylene glycol) (PEG)-silane copolymer [13] were synthesized as previously reported. Electrochemical data were measured with a CHI617B (CH instruments, Inc.; Austin, TX, USA).

2.2. Micropatterning of ITO-Coated Glass Substrates

ITO-coated glass substrates were purchased from Geomatec (Yokohama, Japan). ITO micropatterns on a glass substrate were obtained via standard photolithography and etching processes [40,41]. The ITO-coated glass substrates were sequentially rinsed with acetone, methanol, and distilled water. The cleaned ITO substrates were spin-coated with hexamethyldisilazane as an adhesion promoter and then with AZ5214 as a positive photoresist at 4000 rpm for 30 s. The thickness of the photoresist film was ca. 1.4 μm. The photoresist-coated substrates were soft-baked on a hot plate at 105 °C for 5 min. The substrates were then exposed to UV light in a mask aligner equipped with a patterned mask. The exposed substrates were developed for 90 s. After a rinse with distilled water, the substrates were hard-baked on a hot plate at 110 °C for 2 min. The baked substrates were immersed into an ITO-etching solution for 2 min. Afterward, the remaining photoresist was removed with acetone at 70 °C for 5 min. The patterned ITO glass substrates were diced into smaller sections (2.0 cm × 1.0 cm each). The diced glass substrates were sequentially cleaned with trichloroethylene, ethanol, and distilled water under sonication for 15 min (Figure 1a). The cleaned substrates were pretreated with

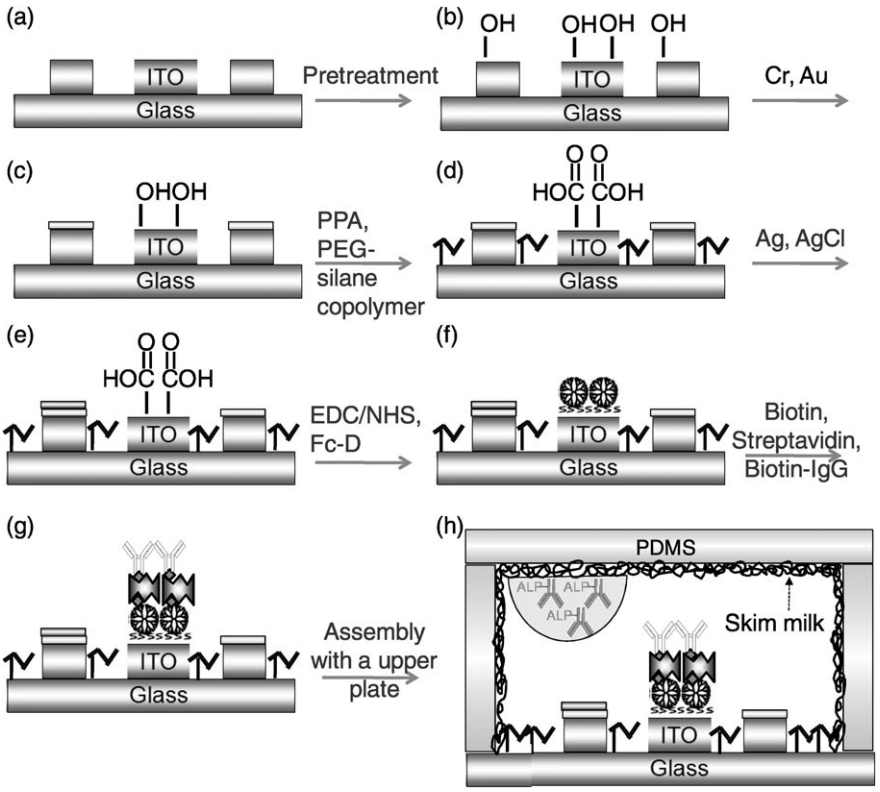

Fig. 1. Schematic diagram that shows the fabrication sequence of an electrochemical immunosensing microchip.

a solution of 5:1:1 H_2O/H_2O_2 (30%)/NH_4OH (30%) at 70 °C for 1.5 h (Figure 1b).

2.3. Fabrication of Reference, Counter, and Working (Sensing) Electrodes

To form a counter and reference electrode on a glass substrate with ITO micropatterns, an Au and Ag/AgCl film were selectively deposited on ITO micropatterns. A Cr film was employed as an adhesion layer for the Au film. To obtain a robust Ag/AgCl film, an Au film on a Cr film was deposited prior to the formation of the Ag/AgCl film. A Cr layer was deposited on two of the three ITO micropatterns by applying −1.0 V for 100 s in an aqueous solution of 10 mM $CrCl_3 \cdot 6H_2O$; an Au layer was then deposited by applying −0.8 V for 50 s in an aqueous solution of 10 mM $HAuCl_4 \cdot 3H_2O$ (Figure 1c). Afterward, one remaining ITO micropattern was selectively modified by immersing the glass substrate in an aqueous solution of 0.1 mM PPA for 36 h at room temperature to generate a carboxylated monolayer (Figure 1d). The glass substrate was immersed in a methanol solution containing 10 mg/mL PEG-silane copolymer for 2 h, followed by curing at 120 °C for 15 min, to form a polymeric silane monolayer on the glass surface not covered with ITO (Figure 1d).

An Ag film was deposited on one out of two Au-coated micropatterns by applying −0.6 V for 50 s in an aqueous solution of 1.0 M NH_3 and 0.3 M $AgSO_4$ (Figure 1e); the glass substrate was then immersed in an aqueous solution of 100 mM $FeCl_3$ for 3 min to convert a portion of the Ag into AgCl (Figure 1e). After being washed with water, the glass substrate was immersed in an aqueous solution containing 50 mM EDC and 25 mM NHS for 2 h to activate the carboxylic acid groups of the PPA-modified ITO micropattern. A methanol solution of 100 μM 2% Fc-D was dropped onto and around the activated ITO micropattern, which was maintained for 2 h (Figure 1f), to attach Fc-D to only the activated ITO micropattern. The Fc-D-attached ITO micropattern was further modified with biotin in a dimethylformamide solution containing 1.5 mg/mL (+)-biotin *N*-hydroxysuccinimide ester for 2 h at 4 °C (Figure 1g). A PBS solution containing 100 μg/mL streptavidin was dropped onto and around the biotin-modified ITO micropattern, which was maintained for 30 min (Figure 1g). The glass substrate was then washed with a RB solution and immersed in a BB solution for 30 min to reduce nonspecific binding of proteins. A PBSB solution containing biotin-IgG was dropped onto and around the streptavidin-modified ITO micropattern, which was maintained for 30 min (Figure 1g); the glass substrate was then washed with RB and PBS. This glass substrate was used as a lower plate of a microchip. The fabricated substrates were stored at 4 °C prior to use.

2.4. Fabrication of an Upper Plate and Its Assembly with a Lower Plate

A master for a patterned PDMS plate was fabricated with a standard soft-lithography procedure [42]. A silicon wafer (6 inch) was used as a substrate for the master. The wafer was cleaned in a piranha solution at 110 °C for 10 min. A photoresist film of KMPR 1050 (Newton, MA, USA) was coated onto the cleaned wafer at 900 rpm for 40 s. The thickness of the film was ca. 105 μm. The substrate was soft-baked in an oven in two steps: 65 °C for 30 min; 95 °C for 120 min. After a relaxation time, the wafer was exposed to UV light at an intensity of 20 mW/cm^2 for 60 s by a mask aligner equipped with a patterned mask. The exposed wafer was post-baked in a baking oven in two steps: 65 °C for 5 min; 95 °C for 15 min. The baked wafer was immersed in a KMPR developer for 15 min and then rinsed with isopropyl alcohol and distilled water. The fabricated master was used to form a patterned PDMS plate. The measured plate thickness was 2.0 mm, and the channel depth was ca. 105 μm. Two solution inlets with 2.0-mm diameter and an air vent with 1.0-mm diameter were formed on the patterned PDMS plate using a puncher. The PDMS plate was immersed in an aqueous solution of 0.1 g/mL skim milk for 2 h to cover the whole surface with skim milk, followed by washing with water. One microliter of a PBSB solution containing 10 μg/mL ALP-IgG was then dropped inside a reaction chamber of the PDMS plate (Figure 1h). This PDMS plate was used as an upper plate of a microchip. Finally, the upper plate (PDMS plate) and the lower plate (glass plate) were assembled (Figure 1h).

3. Results and Discussion

3.1. Selective Modification and Protein-Resistant Surface

The electrochemical biosensing microchip herein consisted of two plates: an upper plate made of a PDMS plate; a lower plate made of an ITO-coated glass (Figure 1h). Micropatterns in the upper plate were designed to control fluid flows and define a reaction chamber where the biochemical reactions occur; micropatterns in the lower plate were designed to provide a biosensing surface and allow electrochemical signaling. Formation of microchannels and a microchamber in the upper plate, and formation of ITO micropatterns in the lower plate, were obtained with the photolithographic process. Selective modification of surfaces with chemicals and biomolecules was achieved by chemical reactivity-controlled patterning and electrochemical deposition. In some cases, to limit the region that the patterning solution contacts, the whole plate was not immersed in the solution: a solution drop was placed onto a region slightly wider than the area where selective surface modification occurs.

For the protein-resistant surface, the PDMS surface in the upper plate was fully coated with skim milk. It is well known that skim milk significantly reduces nonspecific binding of proteins and could block binding sites of immobilized antibodies [43]. Accordingly, skim milk was first coated on bare PDMS; ALP-IgG was then adsorbed onto a part of skim milk-coated PDMS. Figure 2c shows a diagram for relative nonspecific binding of FITC-BSA to bare PDMS, BSA-treated PDMS, Tween 20-treated PDMS, and skim milk-treated PDMS. The skim milk-treated surface showed much less nonspecific binding of FITC-BSA than the BSA- and Tween 20-treated surfaces, indicating that the treatment of skim milk significantly reduces nonspecific binding of proteins on the PDMS surface.

For sandwich-type immunosensing, two target-binding antibodies (biotin-IgG and ALP-IgG) should be micropatterned in a microchip. Biotin-IgG was immobilized on a sensing electrode in the lower plate, whereas ALP-IgG was dropped and dried on the skim milk-coated upper plate. The dried ALP-IgG was readily dissolved into a solution when soaked in a sample solution.

The lower plate contained four different surfaces (working, reference, counter electrode, insulating surface between electrodes). The sequence of a series of selective surface modifications was very important for improved selective modification. First, a counter and a reference electrode were defined by electrodepositing Cr and Au onto two ITO micropatterns. An insulating surface and a working electrode were then differentiated using selective reaction of phosphonate (PPA) with an ITO surface over glass surface. A phosphonate monolayer was selectively formed on the ITO surface, and a polymeric monolayer of PEG-silane copolymer on the unmodified glass surface. Previously from this lab, studies showed that the PEG-silane copolymer was highly resistant to nonspecific protein binding [13]. Afterward, one of the two Cr- and Au-modified ITO surfaces was further modified with Ag and AgCl. The phosphonate-modified ITO surface was selectively modified via several chemical and biospecific reactions to finally form a biosensing working electrode (Figure 1d–g).

Figures 2a and b show XPS spectra of the glass surface and ITO surface, respectively, obtained after a micropatterned ITO-coated glass plate was immersed into a PPA-containing solution. The peak at 129.9 eV in Figure 2b corresponds to the P 2p core-level binding energy, indicating that the ITO surface was modified with a phosphonate layer of PPA. However, the peak was not observed on the glass surface (Figure 2a). These results show that a phosphonate monolayer was formed solely on the ITO surface. It is known that organophosphonates bind to metal oxide and not to silicon oxide surfaces in aqueous solutions [15,16].

3.2. Ag/AgCl Reference Electrode and Au Counter Electrode

Stable microfabricated Ag/AgCl reference electrodes are essential for microchip-based electrochemical biosensors. A new fabrication method for an Ag/AgCl reference

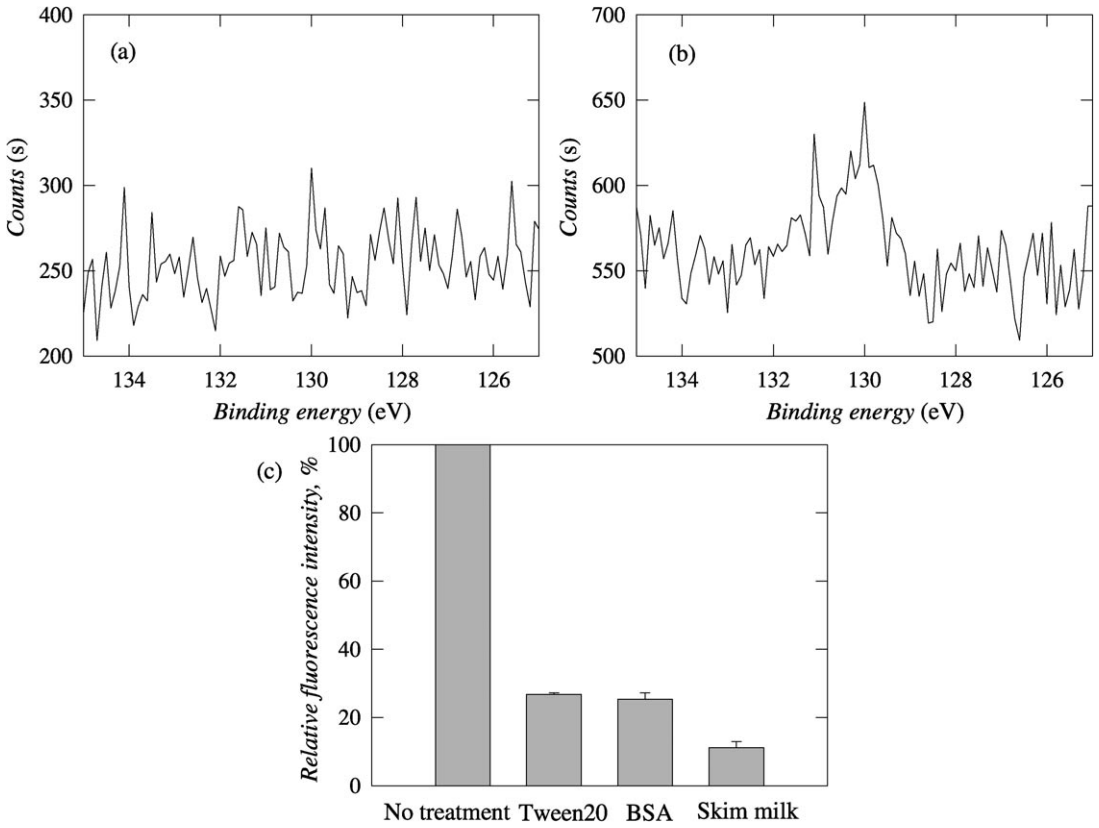

Fig. 2. XPS spectra (for P 2p) of (a) the glass surface and (b) the ITO micropattern obtained after an ITO-micropatterned glass substrate was treated with PPA. (c) Relative nonspecific binding of FITC-BSA to bare PDMS (100% fluorescence intensity), BSA-treated PDMS, Tween 20-treated PDMS, and skim milk-treated PDMS substrate. The PDMS substrate was immersed in a solution of (1 mg/mL) FITC-BSA prior to the measurement of fluorescence intensity. BSA treatment, Tween 20 treatment, and skim milk treatment were performed by immersing a PDMS substrate for 2 h in a solution containing 1% (w/v) BSA, 0.05% (w/v) Tween 20, and 1% (w/v) skim milk, respectively.

electrode on an ITO surface was developed. An Ag film could be directly electrodeposited on the ITO surface. However, such an Ag film was easily removed during the washing process or chemical treatment because Ag adhesion onto the ITO surface was not strong. Even the thick film, electrodeposited for more than 1000 s, was readily stripped off. Moreover, Ag films were not formed well on PPA-modified ITO surface.

Because a stable Ag film on the ITO surface was not obtained, an adhesion layer between the Ag and ITO was considered. An Au adhesion film was electrodeposited on a pretreated ITO electrode. The electrochemical deposition was carried out at −0.8 V for 100, 500, or 1000 s in 10 mM $HAuCl_4$. In all cases, the formed Au film was readily stripped during the washing process (Figure 3b). Moreover, the stability of the Au film worsened after an Ag film formed on the Au film. Perhaps the strong adhesion between the Ag and Au allowed the Au film to be stripped from the ITO surface.

Next, a Cr film was considered as another adhesion layer as Cr is widely used as a stable adhesion layer between metal and metal oxide [25,44]. The electrochemical deposition was carried out at −1.0 V for 100, 500, or 1000 s in 10 mM $CrCl_3$. In all cases, the Cr film was well

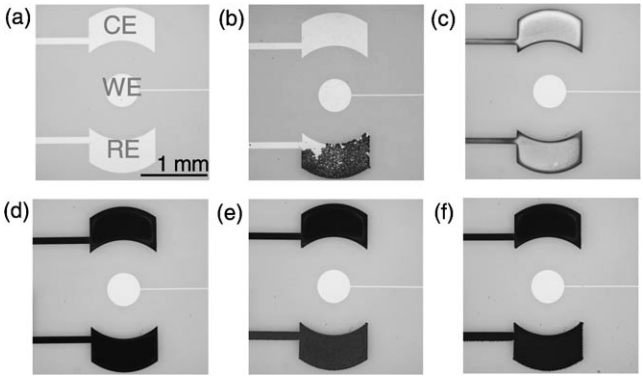

Fig. 3. Optical photographs of ITO micropatterns obtained during microfabrication of an Ag/AgCl reference electrode and an Au counter electrode. The photographs was obtained with (a) unmodified three ITO micropatterns (WE = working electrode, RE = reference electrode, CE = counter electrode) and after (b) Ag electrodeposition on one ITO micropattern (RE only) followed by water washing, (c) Cr electrodeposition on two ITO micropatterns (RE and CE), (d) Au electrodeposition on two Cr-deposited ITO micropatterns (RE and CE), (e) Ag deposition on one Cr- and Au-deposited ITO micropattern (RE only), and (f) AgCl generation in a $FeCl_3$ solution on Cr-, Au-, and Ag-deposited ITO micropattern (RE).

deposited onto the pretreated ITO surface, and the film showed good adhesion stability. However, the Cr film became insulating after lengthy electrodeposition, thereby precluding the deposition of Ag onto Cr. A deposition time of 100 s was optimal for both good adhesion and good electric conductivity. However, because the Ag film that formed on the Cr was not strong enough, the film peeled off during the washing process.

As the adhesion between Au and Cr is known to be good, an additional Au film was used between Cr and Ag film. After a Cr film was electrodeposited at −1.0 V for 100 s on a pretreated ITO electrode (Figure 3c), an Au film was deposited at −0.8 V for 100 s on the Cr/ITO electrode (Figure 3d) and an Ag film at −0.6 V for 100 s on the Au/Cr/ITO electrode (Figure 3e). The formed Ag/Au/Cr/ITO electrode showed very good adhesion stability. Afterward, the Ag/Au/Cr/ITO electrode was immersed in 100 mM $FeCl_3$ for 3 min to convert a portion of the Ag into AgCl (Figure 3f). The final, fabricated Ag/AgCl reference electrode also showed very good adhesion abilities. When the open circuit potential of a fabricated Ag/AgCl reference electrode was measured, a potential drift for 1 h was only a few mV (Figure 4). This result showed that the fabricated Ag/AgCl reference electrode was stable enough to be used as a reference electrode in an electrochemical immunosensing chip. The stability data for the metal films are summarized in Table 1.

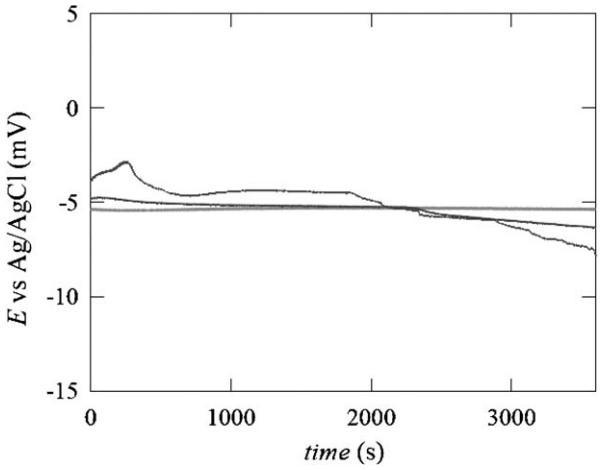

Fig. 4. Open circuit potential of three microfabricated Ag/AgCl reference electrodes measured in 3 M KCl.

3.3. Immunosensing Procedure and Microfluidic Control

The electrochemical immunosensing chip presented herein contained a sample solution inlet (SI), a washing solution inlet (WI), a reaction chamber, a washing valve, an air vent, a working electrode (WE), a reference electrode (RE), and a counter electrode (CE) (Figure 5a). Each component participated in microfluidic control or electrochemical detection. Importantly, no mechanical pumps or valves were used for microfluidic control as

Table 1. Visually observed film state and adhesion stability of electrodeposited metal films on ITO micropatterns.

	Film state	Adhesion
Ag	Good	Bad
Au	Good	Medium
Cr	Medium	Good
Cr (100 s) + Ag	Good	Bad
Cr (500 s) + Ag	Bad	Bad
Cr (1000 s) + Ag	Not formed	Bad
Au + Ag	Good	Bad
Cr (100 s) + Au	Good	Good
Cr (100 s) + Au + Ag	Good	Good

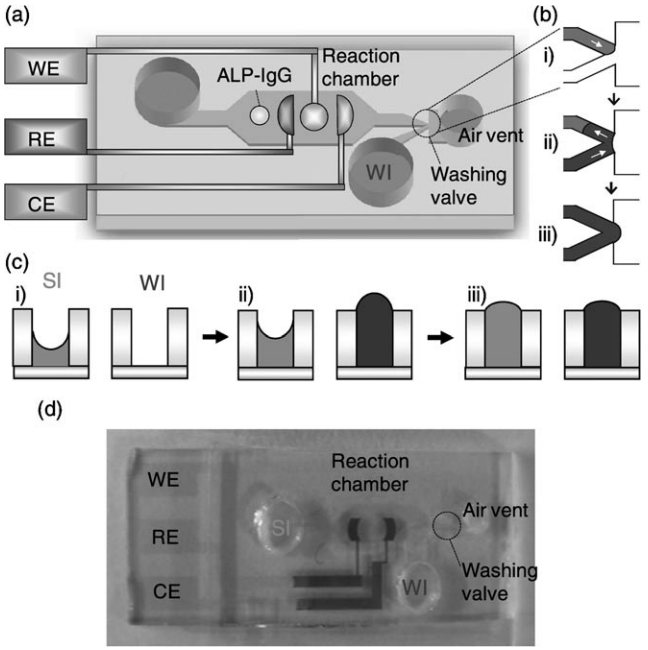

Fig. 5. (a) Schematic diagram of an electrochemical immunosensing microchip. (b) Schematic diagram for solution flow at a washing valve during passive washing. (c) Schematic side view of a sample and a washing solution inlet during passive washing. (d) Photograph of an electrochemical immunosensing microchip.

fluid flows were controlled only by spontaneous capillary-driven flow and passive washing after solution injection. The capillary-driven flow is induced by surface tension of a flowing solution, and the passive washing is due to the pressure difference between the two solutions at the inlets (SI and WI). The initiation of passive washing is controlled by a washing valve. The electrochemical detection employs enzymatic amplification of an electroactive species, followed by its electrochemical oxidation combined with redox cycling.

A sample solution was injected into the SI with a pipette. The solution was drawn into a reaction chamber by capillarity and stopped at a washing valve by the capillary-pressure barrier (i in Figure 5b and c) [33,34]. When the reaction chamber was filled with a sample solution, the ALP-IgG adsorbed on the upper plate (Figure 1h) was dissolved in the solution. When the target mouse IgG

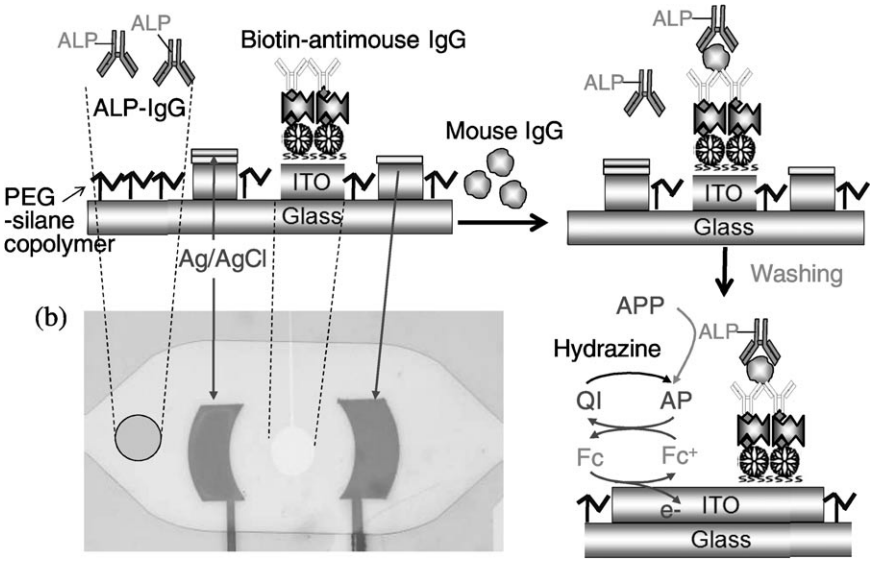

Fig. 6. Schematic diagram that shows sequential biospecific binding processes and electrochemical detection process using enzymatic amplification and redox cycling. (b) Picture of the finally fabricated electrochemical immunosensing chip.

was present in the sample solution, the ALP-IgG bound to the mouse IgG and then to the biotin-IgG on the WE (Figure 6a). The two antigen-antibody reactions were maintained for 10 min. Afterward, a washing solution containing an enzyme substrate and a regent for redox cycling was loaded from the WI by a pipette. When the washing solution merged with the sample solution at a washing valve, the washing solution moved from the WI to SI (ii in Figure 5b) because of the inlet-pressure difference between the two solutions at the SI and WI (ii and iii in Figure 5c). With the help of this solution flow, the sample solution in the reaction chamber was replaced by the washing solution. As a result, the ALP-IgG bound to the WE remained in the reaction chamber while the unbound ALP-IgG was removed from the reaction chamber (Figure 6a). The solution flow maintained until the two inlet pressures equilibrated (iii in Figure 5c). In the reaction chamber, the APP was converted into *p*-aminophenol (AP) by enzymatic reaction of ALP (Figure 6a). After a 10-min incubation, the generated AP was electrochemically measured. The AP was electrooxidized to *p*-quinoneimine (QI) via electromediation of the ferrocene of Fc-D and the QI was reduced back to AP by hydrazine; the AP was then reoxidized electrochemically (Figure 6). The AP redox cycling by hydrazine increased the electrochemical signal in comparison to that in the absence of hydrazine [37].

The inlet pressure is related to the drop shape of the solution at the inlet (Figure 5). Both the optimum volume of the sample solution and the optimum volume of the washing solution are very important in obtaining efficient fluidic flow and passive washing. When the volume was too high, the solution overflowed from the inlet. As long as the solution did not overflow during the solution injection, a highly reproducible drop shape was obtained because the size of the inlet hole limited the meniscus size of the solution drop. Accordingly, the sample solution and the washing solution were controlled not to overflow from the inlets during the injection process (Figure 5c). When the volume of the sample solution was too low, the solution flow could not approach the washing valve. When the volume of the washing solution was too low, the sample solution in the reaction chamber could not be replaced with the washing solution. Experimentally, the optimum volume of the sample solution was 3.0 μL, whereas the optimum volume of the washing solution was 10.0 μL.

Microchannel geometry and washing valve design were executed by considering this lab's previous study [34]. The washing valve was designed to be a V-shaped joint (Figure 5b). The capillary pressure (ΔP_c) of an advancing solution in an expanding rectangular channel is represented by

$$\Delta P_c = -\sigma\left(\frac{\cos\theta_t + \cos\theta_b}{H}\right) - \sigma\left(\frac{\cos(\theta_t+\beta_1) + \cos(\theta_t+\beta_2)}{W}\right) \quad (1)$$

where σ is the surface tension of the solution, θ_t the contact angle of an upper plate, θ_b the contact angle of a lower plate, H the channel height, W the channel width, and β_1 and β_2 the expansion angles [33,34]. They are defined in Figure 7. When a sample solution and a washing solution merge at a washing valve, the merged solution should not flow forward into an air vent. Therefore, ΔP_c should be large enough for a solution to stop and stay at the expanding region without flowing forward into the air vent. When $\theta_t+\beta_1$ and $\theta_t+\beta_2$ are 180°, ΔP_c has a maximum value. Accordingly, $\theta_t+\beta_1$ and $\theta_t+\beta_2$ were designed to be close to 180° both before and after the merging of the two solutions (Figure 7b).

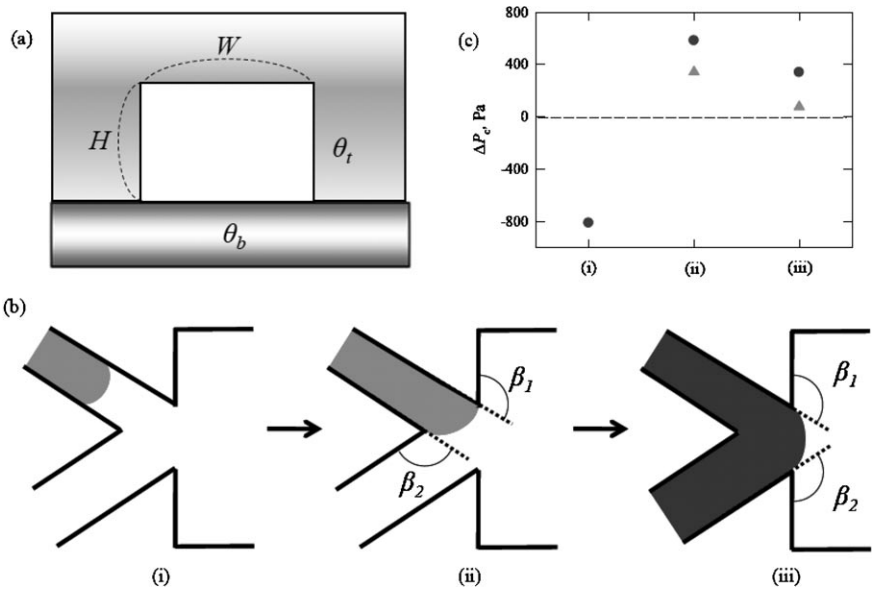

Fig. 7. (a) Schematic of parameters related to geometry and contact angles of a microchannel. (b) Schematic of solution flow (i) just before arriving at the channel-expanding region, (ii) after arriving at the channel expanding region and (iii) after the passive washing. (c) ΔPc calculated from Equation 1 at the regions (i) ($H=105$ μm, $W=89.4$ μm), (ii) ($H=105$ μm, $W=118.8$ μm, $\beta_1=116.6^\circ$, $\beta_1=126.8^\circ$) and (iii) ($H=105$ μm, $W=150$ μm, $\beta_1=116.6^\circ$, $\beta_1=116.6^\circ$) ($\theta_t=73^\circ$ and 60.6° at 10 s and 10 min, respectively; $\theta_b=61.6^\circ$ and 39.5° at 10 s and 10 min, respectively). Circle data were obtained using the values of contact angle measured at 10 s after a solution is dropped, whereas triangle data were obtained using the values of contact angle at 10 min.

Since the contact angle of a solution on a solid surface generally decreases with time, the ΔP_c at a washing valve should be calculated by considering both the initial contact angle and the contact angle after an extended period of time. Accordingly, two contact angles at 10 s and 10 min were measured after a PBSB solution was dropped on the skim milk-coated PDMS surface and the glass surface modified with the PEG-silane copolymer. The contact angle of the PDMS surface was $73\pm1.9^\circ$ and $60.6\pm4.1^\circ$ at 10 s and 10 min, respectively; the contact angle of glass surface was $61.6\pm3.3^\circ$ and $39.5\pm2.9^\circ$ at 10 s and 10 min, respectively. The ΔP_c calculated from these values is shown in Figure 7b. The ΔP_c was positive enough, even when the solution stays at the expanding region for 10 min. The ΔP_c at the washing valve was sufficient for the solution to cease and remain at the valve without flowing forward into the air vent.

3.4. Immunosensing Performance

The dependence of the cyclic voltammograms on the mouse-IgG concentration is shown in Figure 8. The redox current is associated with AP oxidation and background current. Figure 9 shows a cyclic voltammogram obtained at an Fc-D-modified microfabricated electrode in a microchip. The redox peak around 0.2 V is related to a ferrocene redox reaction, which helps electromediated oxidation of AP. As the concentration of mouse IgG increased, the current of AP oxidation increased in the cyclic voltammograms (Figure 8). Because of AP redox cycling by hydrazine, cyclic voltammograms showed a mixed behavior of a plateau-shaped curve and a peak-shaped curve [37]. All anodic peaks in the cyclic voltammograms appeared at similar potentials, and the cyclic voltammograms were quite reproducible. These results indicate that the microfabricated Ag/AgCl reference electrode worked stably and reproducibly.

The immunosensing response obtained at a mouse-IgG concentration of zero, without using ALP-IgG, was measured to compare with the response obtained with using ALP-IgG (Figure 9b). The difference between the two responses is attributed to the level of nonspecific binding of ALP-IgG and the efficiency of passive washing. The current near 0.2 V (near a peak potential of ferrocene) in the cyclic voltammogram using ALP-IgG was slightly higher than without ALP-IgG. If the level of nonspecific binding of ALP-IgG was high in a reaction chamber and the unbound ALP-IgG not fully removed from a reaction chamber by passive washing, the current from using ALP-IgG would be much higher than without ALP-IgG. These results clearly show that the level of nonspecific binding of proteins was very low and that the passive washing is very effective.

At a mouse-IgG concentration of 10 pg/mL, the current at 0.23 V was 13.6 ± 1.8 nA (mean $\pm$ standard deviation), which was much higher than in the absence of the mouse IgG (6.3 ± 1.9 nA). Figure 8d represents the calibration curve for currents at 0.23 V in a range of concentrations from 10 pM to 10 μM. The calculated detection limit of the presented electrochemical immunosensing chip was ca. 10 pg/mL for mouse IgG, indicating that the electrochemical immunosensor was highly sensitive and reproducible.

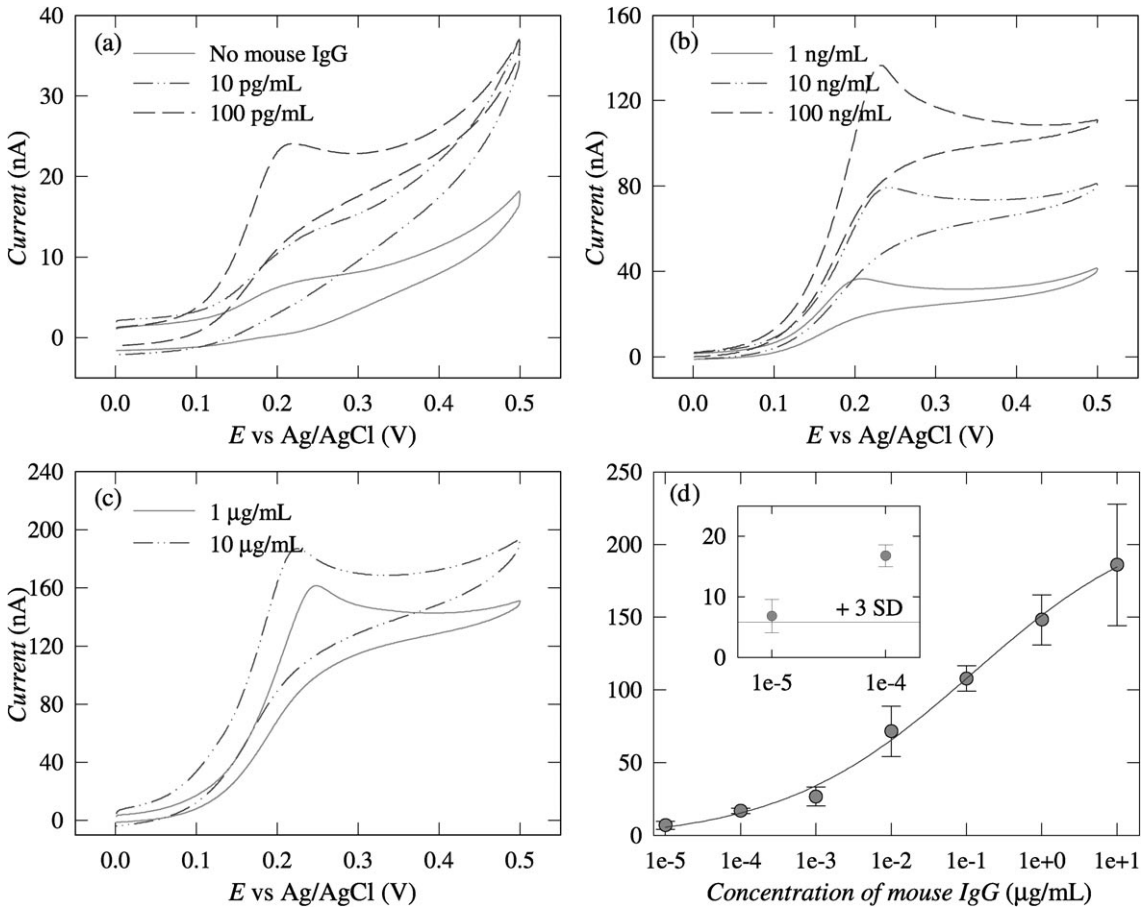

Fig. 8. (a–c) Dependence of cyclic voltammograms on the concentration of mouse IgG. The cyclic voltammograms were obtained in a microchip 10-min after passive washing with a tris buffer solution (pH 9.0) containing 1 mM APP and 10 mM hydrazine at a scan rate of 50 mV/s. (d) Calibration curve for an electrochemical immunosensor. All current data obtained at 0.23 V were subtracted by the mean current at a concentration of zero. The inset represents a magnification of the graph at low concentrations. The dashed line corresponds to three times the standard deviation (SD) at zero concentration.

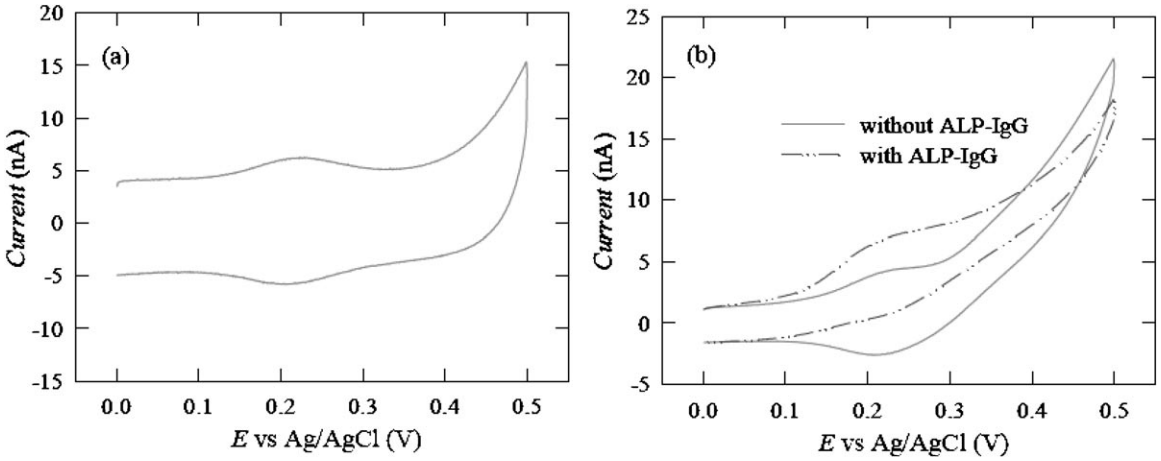

Fig. 9. (a) Cyclic voltammogram of a 2% Fc-D-modified micropatterned ITO electrode in Tris buffer (pH 9.0) at a scan rate 50 mV/s and (b) cyclic voltammograms obtained at a mouse-IgG concentration of zero in the presence or absence of ALP-IgG in a microchip 10 min after passive washing with a Tris buffer solution (pH 9.0) containing 1 mM APP and 10 mM hydrazine at a scan rate of 50 mV/s.

4. Conclusions

A sensitive electrochemical immunosensing microchip has been developed using new microfabrication methods, capillary-driven microfluidic control, and signal amplification by redox cycling. Selective modification of the surfaces was achieved by a proper combination of different protein-resistant surfaces and their sequential selective modification. The stability of a microfabricated Ag/AgCl reference electrode was improved using an adhesion layer of Cr and Au on the ITO surface. Microfluidic control was achieved by spontaneous capillary-driven flows and passive washing; a high electrochemical signal was obtained by redox cycling combined with enzymatic amplification. The level of nonspecific binding of proteins was so low, and the passive washing so effective that a detection limit of 10 pg/mL for mouse IgG was achieved. It seems that the new microfabrication procedure and the combination of capillary-driven microfluidic control with electrochemical detection could be practically applied to a portable biosensing device for point-of-care testing.

Acknowledgements

This work was supported by the Basic Science Research Program through the *National Research Foundation* (*NRF*) (2009-0085182 and 2009-0072062) and the Nano/Bio Science & Technology Program (2005-01333) of the *Ministry of Education, Science and Technology* (*MEST*).

References

[1] A. Bange, H. B. Halsall, W. R. Heineman, *Biosen. Bioelectron.* **2005**, *20*, 2488.
[2] J. Wang, *Electroanalysis* **2005**, *17*, 1133.
[3] J. Wang, M. Pumera, M. P. Chatrathi, A. Rodriguez, S. Spillman, R. S. Martin, S. M. Lunte, *Electroanalysis* **2002**, *14*, 1251.
[4] M. Pumera, A. Merkoçi, S. Alegret, *Trends Anal. Chem.* **2006**, *25*, 219.
[5] M. Mir, A. Homs, J. Samitier, *Electrophoresis* **2009**, *30*, 3386.
[6] X. Xu, S. Zhang, H. Chen, J. Kong, *Talanta* **2009**, *80*, 8.
[7] J.-J. Xu, A.-J. Wang, H.-Y. Chen, *Trends Anal. Chem.* **2007**, *26*, 125.
[8] B. Hongyan, W. Zhong, S. Meng, J. Kong, P. Yang, B. Liu, *Anal. Chem.* **2006**, *78*, 3399.
[9] T. Matsumoto, A. Ohashi, N. Ito, *Anal. Chim. Acta* **2002**, *462*, 253.
[10] H.-X. Ren, X.-J. Huang, J.-H. Kim, Y.-K. Choi, N. Gu, *Talanta* **2009**, *78*, 1371.
[11] N. Gomez, J. Y. Lee, J. D. Nickels, C. E. Schmidt, *Adv. Funct. Mater.* **2007**, *17*, 1645.
[12] P. Jonkheijm, D. Weinrich, H. Schröder, C. M. Niemeyer, H. Waldmann, *Angew. Chem. Int. Ed.* **2008**, *47*, 9618.
[13] M. A. Aziz, S. Park, S. Jon, H. Yang, *Chem. Commun.* **2007**, *25*, 2610.
[14] K. Hofmann, G. Titus, J. A. Montibeller, F. M. Finn, *Biochemistry* **1982**, *21*, 978.
[15] P. H. Mutin, V. Lafond, A. F. Popa, M. Granier, L. Markey, A. Dereux, *Chem. Mater.* **2004**, *16*, 5670.
[16] R. Michel, J. W. Lussi, G. Csucs, I. Reviakine, G. Danuser, B. Ketterer, J. A. Hubbell, M. Textor, N. D. Spencer, *Langmuir* **2002**, *18*, 3281.
[17] U. Plutowski, S. S. Jester, S. Lenhert, M. M. Kappes, C. Richert, *Adv. Mater.* **2007**, *19*, 1951.
[18] S. Jon, J. Seong, A. Khademhosseini, T.-N. T. Tran, P. E. Laibinis, R. Langer, *Langmuir* **2003**, *19*, 9989.
[19] M. G. Roper, J. G. Shackman, G. M. Dahlgren, R. T. Kennedy, *Anal. Chem.* **2003**, *75*, 4711.
[20] J. Kong, L. Jiang, X. Su, J. Qin, Y. Du, B. Lin, *Lab Chip* **2009**, *9*, 1541.
[21] H.-J. Kim, K. C. Ahn, A. González-Techerab, G. G. González-Sapienzab, S. J. Geea, B. D. Hammocka, *Anal. Biochem.* **2009**, *386*, 45.
[22] Y. Wan, J. Zhang, G. Liu, D. Pan, L. Wang, S. Song, C. Fan, *Biosens. Bioelectron.* **2009**, *24*, 1209.
[23] M. L. Pourciel-Gouzy, S. Assié-Souleillea, L. Mazenqa, J. Launaya, P. Temple-Boyera, *Sens. Actuators B* **2008**, *134*, 339.
[24] H. Suzuki, H. Shiroishi, S. Sasaki, I. Karube, *Anal. Chem.* **1999**, *71*, 5069.
[25] B. J. Polk, A. S. Stelzenmuller, G. Mijares, W. MacCrehan, M. Gaitan, *Sens. Actuators B* **2006**, *114*, 239.
[26] A. Hiratsuka, K. Ikebukuro, I. Karube, K. Kojima, H. Suzuki, H. Muguruma, *Analyst* **2001**, *126*, 658.
[27] G. Ocvirk, M. Munroe, T. Tang, R. Oleschuk, K. Westra, D. J. Harrison, *Electrophoresis* **2000**, *21*, 107.
[28] A. Dodge, K. Fluri, E. Verpoorte, N. F. de Rooij, *Anal. Chem.* **2001**, *73*, 3400.
[29] J. S. Ko, H. C. Yoon, H. Yang, H.-B. Pyo, K. H. Chung, S. J. Kim, Y. T. Kim, *Lab Chip* **2003**, *3*, 106.
[30] D. Junker, H. Schmid, U. Drechsler, H. Wolf, M. Wolf, B. Michel, N. de Rooji, E. Delamarche, *Anal. Chem.* **2002**, *74*, 6139.
[31] L. Gervais, E. Delamarche, *Lab Chip* **2009**, *9*, 3330.
[32] J. C. T. Eijkel, A. V. D. Berg, *Lab Chip* **2006**, *6*, 1405.
[33] S.-J. Kim, Y. T. Lim, H. Yang, Y. B. Shin, K. Kim, D.-S. Lee, S. H. Park, Y. T. Kim, *Anal. Chem.* **2005**, *77*, 6494.
[34] B.-K. Kim, S.-J. Kim, S.-Y. Yang, H. Yang, *J. Micromech. Microeng.* **2007**, *17*, N22.
[35] Y. T. Lim, S.-J. Kim, H. Yang, K. Kim, *J. Micromech. Microeng.* **2006**, *16*, N9.
[36] J. Das, M. A. Aziz, H. Yang, *J. Am. Chem. Soc.* **2006**, *128*, 16022.
[37] J. Das, K. Jo, J. W. Lee, H. Yang, *Anal. Chem.* **2007**, *79*, 2790.
[38] M. A. Aziz, S. Patra, H. Yang, *Chem. Commun.* **2008**, *38*, 4607.
[39] J. Das, H. Kim, K. Jo, K. H. Park, S. Jon, K. Lee, H. Yang, *Chem. Commun.* **2009**, 6394.
[40] Y. Xia, G. M. Whitesides, *Annu. Rev. Mater. Sci.* **1998**, *28*, 153.
[41] D. Brambley, B. Martin, P. D. Prewett, *Adv. Mater. Opt. Electron.* **1994**, *4*, 55.
[42] J. C. McDonld, D. C. Duffy, J. R. Anderson, D. T. Chiu, H. Wu, O. G. A. Schueller, G. M. Whitesides, *Electrophoresis* **2000**, *21*, 27.
[43] R. T. Miller, P. Kubier, B. Reynolds, T. Henry, H. Turnbow, *Appl. Immunohisto. M. M.* **1999**, *7*, 63.
[44] E. W. H. Jager, E. Smela, O. Inganäs, *Science* **2000**, *290*, 1540.

